

# Collinear Ternary Cluster Decay of Hyper-deformed $^{60}\text{Zn}$ at High Angular Momentum

V. I. Zherebchevsky<sup>+\*∇1)</sup>, W. von Oertzen<sup>\*∇</sup>, D. V. Kamanin<sup>□</sup>

<sup>+</sup>St. Petersburg University, 198504 St. Petersburg, Russia

<sup>\*</sup>Hahn-Meitner-Institut-GmbH, D-14109 Berlin, Germany

<sup>∇</sup>Fachbereich Physik, Freie Universität, 14195 Berlin, Germany,

<sup>□</sup>Flerov laboratory for Nuclear Reactions, 141980 Dubna, Russia

Submitted 6 October 2006

Resubmitted 26 December 2006

Binary and ternary cluster decay of  $^{60}\text{Zn}$  compound nuclei at high angular momentum, formed in the  $^{36}\text{Ar} + ^{24}\text{Mg}$  reaction at  $E_{\text{lab}}(^{36}\text{Ar}) = 195$  MeV, has been measured in a unique kinematic coincidence setup consisting of two large area position sensitive  $(x, y)$  gas detector telescopes with Bragg-ionisation chambers (BRS). The BRS gives the opportunity to measure the reaction angles in- and out-of-plane, and through Bragg-curve spectroscopy to achieve a complete identification of the nuclear charge for different final channels. We observed very narrow out-of-plane angular correlations for two heavy fragments emitted in either purely binary events or in events with a missing mass consisting of 2 and 3  $\alpha$ -particles. These narrow correlations are interpreted as ternary fission decay from compound nuclei at high angular momenta through an elongated (hyper-deformed) shape with very large moment of inertia. In these stretched configurations the lighter mass in the neck region remains at rest or with very low momentum in the center of mass.

PACS: 25.60.Dz, 25.70.Gh, 27.50.+e

For composite system in the light mass region  $A_{CN} \leq 60$ , the fusion-fission process is an important channel in the compound nucleus (CN) decay. Of particular interest are the decays from deformed shapes (super- and hyper-deformed) of  $N = Z$  nuclei. In fission the saddle point configurations become strongly elongated with smaller CN mass (decreasing fission parameter), and a ternary fission process may be observed. In addition, a collinear ternary fission decay is expected for the highest angular momentum, and we will have a stretched configuration of the formed fragments [1]. Using a generalized liquid drop model, taking into account the proximity energy and quasi-molecular shapes (as in the cluster models) [2, 3], the ternary fission process from the hyper-deformed configuration is expected, and will be enhanced due to a lowering of the corresponding fission barriers at high angular momentum. An additional lowering of the barrier by shell corrections is predicted in many calculations, based mainly on the Nilsson-Strutinsky method [4–9]. The energetically favoured shape for quadrupole deformation and for the hyper-deformed configuration correspond to major-to-minor axis ratios of 3:1. These shapes are stabilized due

to quantal effects and represent configurations, which are several MeV lower than the liquid drop fission barrier. The ternary fission decay competes with the binary fission due to the formation of these strongly deformed configurations.

The present research is a study of collinear ternary decay of the hyper-deformed  $^{60}\text{Zn}$  compound nucleus at an excitation energy of  $E_{ex} = 88$  MeV, formed in the  $^{36}\text{Ar} + ^{24}\text{Mg}$  reaction at a bombarding energy of  $E_{\text{lab}}(^{36}\text{Ar}) = 195$  MeV. The maximum angular momentum reached for  $^{60}\text{Zn}$  is close to  $(48-50)\hbar$ , consistent with the predicted liquid drop limit [10]. The experiment was performed at the ISL facility at the HMI Berlin with the Binary Reaction Spectrometer (BRS) [11, 12]. The beam was pulsed with a time resolution of 1 ns, and high spatial resolution. The BRS consisted of two large area heavy ion detector telescopes (labeled 3 and 4), positioned on either side of the beam direction. Both detector telescopes have two-dimensional position and time-of-flight (TOF) sensitive low-pressure multi-wire chambers (MWC), Bragg-curve Ionization Chambers (BIC), and all detection planes are electrically four-fold segmented in order to improve the resolution. With the BRS it is possible to measure two heavy fragments in coincidence with respect to their in-plane  $(\theta_3, \theta_4)$ , and

<sup>1)</sup>e-mail: vozhereb@mail.ru

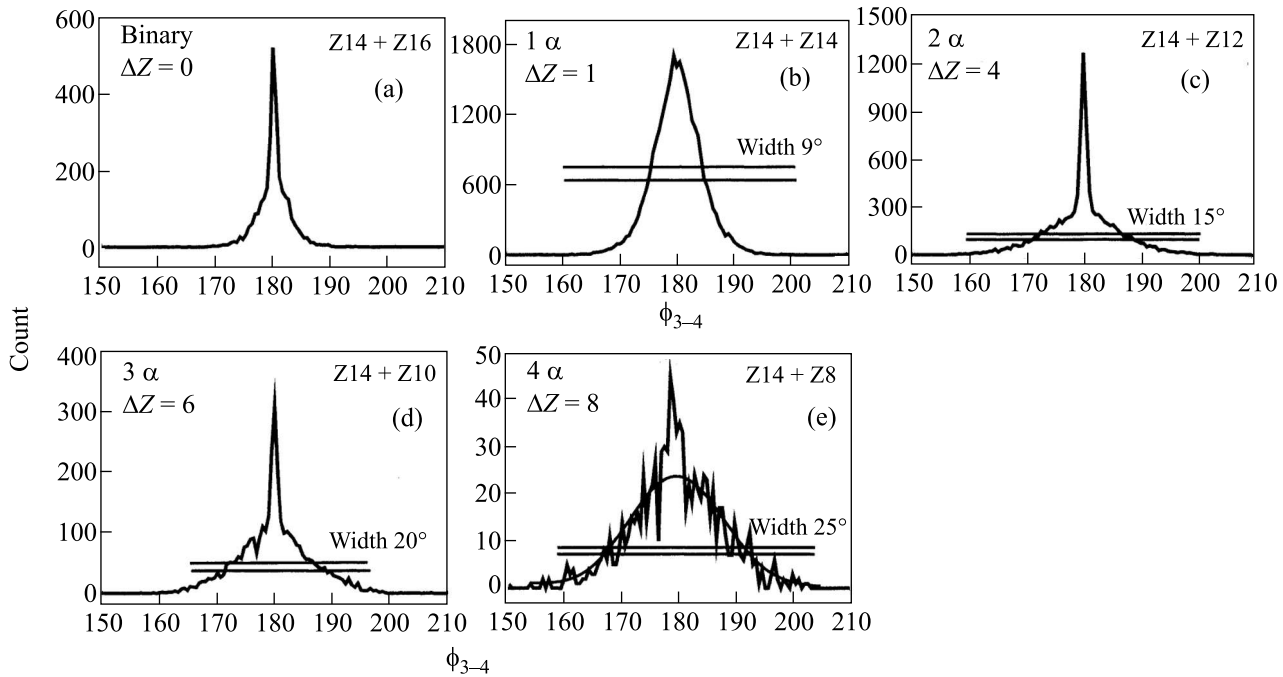


Fig.1. Out-of-plane  $\varphi_{3-4}$  angular correlations of coincident fragments with charges  $Z_3$  and  $Z_4$ . The yields are as follows for: (a) binary decay, (b) binary decay with  $1\alpha$ -emission, (c) decay with  $2\alpha$ -emission, (d) decay with  $3\alpha$ -emission, (e) decay with  $4\alpha$ -emission as indicated. The width of broad component for different fission channels are shown

out-of-plane scattering angles ( $\varphi_3$ ,  $\varphi_4$ ), time of flight (TOF) and energy ( $E$ ). In comparison to previous works [13,14] these coincidences represent an exclusive measurements of the binary fission yield. The Bragg-curve spectroscopy is used for a complete coverage of the charge yields in the different final channels. In the present reaction:  $^{36}\text{Ar} + ^{24}\text{Mg} \rightarrow (\text{CN}, ^{60}\text{Zn}^*) \rightarrow (M_3 Z_3) + (\Delta Z) + (M_4 Z_4)$ , both heavy fragments with masses ( $M_3$ ,  $M_4$ ) and charges ( $Z_3$ ,  $Z_4$ ) are registered in kinematical coincidence and identified by their charges.

Charge separation in the BIC's has been applied by using corresponding gates on BP-E distributions for each charge. Choosing the gates for different charges and using correlations for  $Z_3$  (charge obtained in the first detector) –  $Z_4$  (charge obtained in the second detector), the individual binary and non binary reaction channels can be clearly identified. Fission channels are defined by the sum of the observed charges of the fragments, registered in coincidence, with missing charge  $\Delta Z = Z_{\text{total}} - (Z_3 + Z_4)$  – the charge of the compound nucleus minus the sum of the charges of detected fragments.

After selection of channels via the ( $Z_3$ ,  $Z_4$ ) correlations we have unique results for the out-of-plane angular correlations,  $\varphi_{3-4}$ , for different missing charges  $\Delta Z$ . As expected in the pure binary cases ( $\Delta Z = 0$ , fragments are only registered up to their  $\alpha$ -particle decay thresh-

olds), the out-of-plane correlation is sharp, except for a small broader second component resulting from neutron evaporation, see Fig.1a. For sequential  $\alpha$ -particle emission one would expect broader correlations with increasing width for increasing missing charges. This is fulfilled for missing charges  $\Delta Z = 2$ , see Fig.1b. These events are originally binary fission with an excitation energy in either fragment sufficiently high for one  $\alpha$ -particle to be emitted. However, for missing charges of  $\Delta Z = 4, 6$  a strong narrow component, as in the binary cases, was found together with a second broad component, see Figs.1c, d. The origin of these two components can be described with different fission mechanisms, as will be discussed below.

In the  $^{36}\text{Ar} + ^{24}\text{Mg}$  reaction, a compound nucleus,  $^{60}\text{Zn}$ , is formed. Apart from the statistical decay with light particles emission, we can have different fission decay channels:

1. Binary fission decay of the compound system: two heavy fragments are formed ( $Z_3 + Z_4 = Z_{\text{CN}}$ ) with their excitation energies below the  $\alpha$ -particle decay thresholds, this process we call pure binary decay.

2. A fission process, where 1–4  $\alpha$  particles are emitted from the fully accelerated fragments, resulting in the broad components in out-of-plane angular correlations,  $\varphi_{3-4}$  for  $\Delta Z = 2-8$ . In momentum space the fragments after  $\alpha$  emission have a kinematical angular cone

of scattering. We will call this process – the binary with statistical  $\alpha$ -particle emission.

3. A ternary fission process (from a strongly deformed state at high angular momentum, of about  $48 \hbar$ ) with  $\Delta Z = 4-8$ . For this ternary fission the emission of the  $\alpha$ -cluster structure from the neck area is expected.

These ternary fragments are formed by 2 or 3  $\alpha$  particles, and are expected to have very low momentum or are at rest in the in the centre of mass(cm)-frame of the CN. Assuming that the prompt ternary fission process has a negligible probability, we will make in the following the assumption of a sequential decay process. In order to have a model for the kinematics of the ternary fragment, we assume that the  $\alpha$ -cluster structure in the neck is emitted “backwards” from one of the moving fragments, and thus finally obtains a small (or zero) value of its momentum in the cm-frame of the CN. The narrow width components in Figs.1c and d around  $\varphi_3 + \varphi_4 = 180^\circ$  (coplanarity condition), can be understood with such a formation of the missing charges in the neck. Looking at the total kinetic energy (TKE) we find that this process produces in the narrow  $\varphi_{3-4}$ -TKE correlation a much higher value of TKE, then the average value obtained with the statistical  $\alpha$  emission in all directions. The detailed analysis of this mechanism will be discussed below.

For the narrow component we have to discuss the contribution from contaminants in the target. This is a very important question because our effect observed in the out-of-plane distributions could be explained as a binary decay of a compound system formed with  $^{16}\text{O}$  instead of a processes of the ternary fission from  $^{60}\text{Zn}$ . In the present case it will be the  $^{16}\text{O} + ^{36}\text{Ar}$  reaction for the  $\Delta Z = 4$  channel (ternary fission mechanism), and  $^{12}\text{C} + ^{36}\text{Ar}$  for the  $\Delta Z = 6$  channel. Therefore we must estimate the probability of reactions with  $^{16}\text{O}$  and  $^{12}\text{C}$  nuclei. We have four points, which show, that the reactions are not due to  $^{16}\text{O}$  or  $^{12}\text{C}$  in the target (a contribution of 15 % is estimated). All calculations have been done by transformation into the center of mass frame.

1. Estimations of the target thickness. For the target thickness determination of the  $^{16}\text{O}$  component, we used the relation of the differential cross-section of the narrow part (assuming binary for  $^{16}\text{O}$ ) in the yield with missing charge  $\Delta Z = 4$ , to the differential cross-section for the pure binary decay (binary for  $^{24}\text{Mg}$ ) with  $\Delta Z = 0$ . If we assume that the narrow peak in the out-of-plane distribution for the  $\Delta Z = 4$  case, arises due to reaction on the  $^{16}\text{O}$ , it was found, that two times more  $^{16}\text{O}$  is needed than is possible for a completely oxidized  $^{24}\text{Mg}$ -target (only a 10% contribution due to the oxidation is expected).

2. Analysis of the ratios of differential cross-sections for the different missing charge combinations. From the out-of-plane distributions (see Fig.1a, b) we have calculated the ratio of differential cross-section of binary process with  $1\alpha$  emission ( $^{36}\text{Ar} + ^{24}\text{Mg} \rightarrow ^{28}\text{Si} + ^{28}\text{Si} + 1\alpha$ ) to the differential cross-section of the pure binary process ( $^{36}\text{Ar} + ^{24}\text{Mg} \rightarrow ^{28}\text{Si} + ^{32}\text{S}$ ), and the same for the  $^{16}\text{O}$  case. We have found, that the yield in the broad distribution (see Fig.1b) is 8 times stronger than the yield of the pure binary reaction. Then we have considered a reaction, where the narrow part in  $\Delta Z = 4$  could arise from the interaction  $^{36}\text{Ar}$  with  $^{16}\text{O}$  (Fig.1c – binary case):  $^{36}\text{Ar} + ^{16}\text{O} \rightarrow ^{28}\text{Si} + ^{24}\text{Mg}$ , and for a  $1\alpha$  emission ( $^{36}\text{Ar} + ^{16}\text{O} \rightarrow ^{28}\text{Si} + ^{20}\text{Ne} + 1\alpha$ , Fig.1d, broad part). The observed yield in the broad part in  $\Delta Z = 6$  should be at least 8 times stronger, but the experimental results show a very small broad component, which is a factor 10 to small to originate from  $^{16}\text{O}$ . Hence, in this case the  $^{36}\text{Ar} + ^{24}\text{Mg}$  reaction is dominating. A similar argument has been applied for  $^{12}\text{C}$  in the target (see Fig.1d, e). It has been concluded that the contribution to  $\Delta Z = 8$  (very small broad component – a factor 18) to be due to the  $^{36}\text{Ar} + ^{12}\text{C}$  reaction is too small (a contribution of 15% from  $^{12}\text{C}$  to the narrow component in  $\Delta Z = 6$  is estimated).

3. The width of the out-of-plane distributions for the binary decays with  $\alpha$ -emission. For the binary decay (reaction on  $^{24}\text{Mg}$  target) with sequential emission we expect the broad out-of-plane correlations to have an increasing width for increasing missing charges. This is fulfilled for the distributions with missing charges  $\Delta Z = 2, 4, 6$  and  $8$ . The width increases from  $9^\circ$  ( $\Delta Z = 2$ ),  $15^\circ, 21^\circ$  to  $25^\circ$  for  $\Delta Z = 8$ , see Fig.2, respectively. This fact shows that the observed broad components are connected to the  $^{36}\text{Ar} + ^{24}\text{Mg} \rightarrow ^{28}\text{Si} + ^{24}\text{Mg} + X\alpha$  reaction, where  $X\alpha$ -particles are emitted statistically from excited fragments.

4. Analysis of the in-plane angular distributions ( $\theta_3$  vs.  $\theta_4$ ). The analysis of two dimensional ( $\theta_3, \theta_4$ ) correlations has been done together with the kinematical calculations for the two reactions, where the targets are either  $^{16}\text{O}$  or  $^{24}\text{Mg}$ . Using a gate applied in the TKE-out-of-plane correlation, we have taken only those events, which produced the narrow part. Then, we calculated the kinematical curves for the same fragments ( $Z_3 = 14, Z_4 = 12$ ), formed in the  $^{36}\text{Ar} + ^{16}\text{O}$  and  $^{36}\text{Ar} + ^{24}\text{Mg}$  reactions, respectively. We use an excitation energy  $E_{ex}$  of the fragments in the  $^{36}\text{Ar} + ^{16}\text{O}$  reaction with  $E_{ex} \approx 10$  MeV (where  $Q_{\text{eff}} = Q_0 + E_{ex}$ ), and  $E_{ex}$  is below the decay threshold, but allowing mutual excitation. These events correspond to regions where the strongest contribution of the reactions on  $^{16}\text{O}$  are

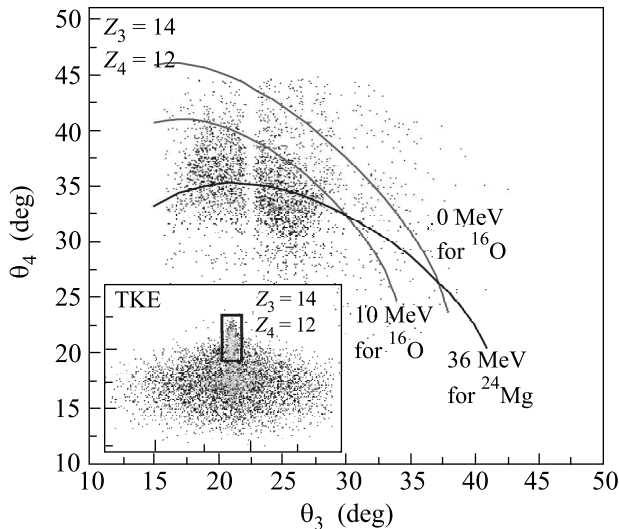


Fig.2. Two dimensional plot of  $\theta_3$  vs.  $\theta_4$  with calculated kinematical curves for two detected fragments  $Z_3, Z_4$  from  $^{36}\text{Ar}+^{16}\text{O}$  (fragment excitation energy  $E_{ex} = 10$  MeV) and  $^{36}\text{Ar}+^{24}\text{Mg}$  ( $E_{ex} = 36$  MeV) reactions. The experimental yield obtained with a gate set for the narrow part in out-of-plane vs. TKE distribution (insert)

expected. The kinematical curve lies in the border of experimental events in the two-dimensional angular distribution, see Fig.2. In the region with a further increase of the excitation energy ( $E_{ex} \approx 20$  MeV), fragments will emit  $\alpha$ -particles, and the experimental yield of the  $\theta_3$  vs.  $\theta_4$  distribution can not anymore correspond to the chosen reaction exit channel ( $Z_3 = 14, Z_4 = 12$ ) on  $^{16}\text{O}$ .

For the  $^{36}\text{Ar} + ^{24}\text{Mg}$  reaction we will not have the restrictions in the excitation energy area, because the reaction channel ( $Z_3 = 14, Z_4 = 12$ ) has high excitation energy in each fragment to allow evaporation of two  $\alpha$ -particles ( $E_{ex}$  is  $\approx 36$  MeV). For this reaction, the kinematical curve is in good agreement with the experimental data (Fig.2), where the main intensity of registered events are located.

For the discussion of the fission mechanism we must consider the formation and the decay of the compound nucleus at the highest angular momenta, see also [15]. We have a three-body configuration which produces the narrow component in the  $(\phi)$  correlations at  $|\phi_3 + \phi_4| = 180^\circ$ . Three fragments could be placed at different relative orientations. In ref. [1] it has been shown, that for small angular momenta a triangular configuration is favored, while for higher angular momenta the decay system has a stretched configuration caused by centrifugal forces. In our case the  $^{60}\text{Zn}$  compound nucleus decays with  $2\alpha$  or  $3\alpha$  clusters formed in the neck, – the missing  $\alpha$ -particles must be placed between the two heavier fission fragments. This decay may go

through two phases: the first – the decay of the compound system in two fragments, the second – a sequential  $\alpha$ -cluster emission from one of the fragments:  $A + a \rightarrow B + (b + (2\alpha, 3\alpha))$ , see Fig.3a. As discussed

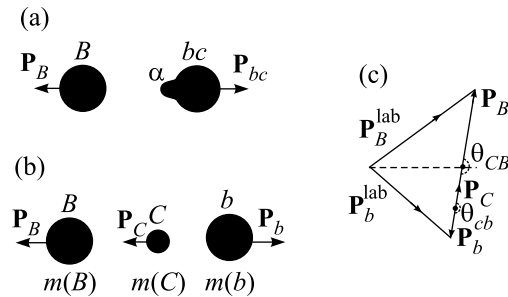


Fig.3. Ternary decay as a consecutive two-steps fission process. The first phase – (a), is a binary decay of the compound system in two fragments  $B + bc$ . The second – (b), (c) –  $\alpha$  cluster emission from one of the fragments

before for our narrow out-of-plane distributions, the reaction mechanism can be modeled with the  $\alpha$ -clusters emitted “backwards” from one of the moving heavier fragments (the angle between fragments remains  $180^\circ$ ), as shown at the Fig.3b.

We consider the kinematics of the second phase in the sequential cluster emission after fission, when the ternary clusters are emitted, see Fig. 3 b, c. We define  $\mathbf{P}_B, \mathbf{P}_{bc}, \mathbf{P}_b$ , and  $\mathbf{P}_C$  as the momenta (in the center of mass frame) of the first primary fragment –  $B$ , of the second primary fragment –  $bc$ , of the final fragment  $b$  (after cluster emission) and of the ternary cluster –  $C$ , correspondingly. Analogous we define:  $E_B, E_b, E_C$  – the kinetic energies in the exit channel. The energy conservation for present reaction is:  $E_B + E_b + E_C = E_{cm} + Q$ .

The conservation of the linear momentum in the cm frame for the second phase gives:  $\mathbf{P}_B + \mathbf{P}_b + \mathbf{P}_C = 0$ . Then the kinetic energy of the fragment  $b$  is:

$$E_b = \frac{(\mathbf{P}_B + \mathbf{P}_C)^2}{2m(b)} = \frac{\mathbf{P}_B^2 + \mathbf{P}_C^2 + 2\mathbf{P}_B\mathbf{P}_C}{2m(b)} = \frac{m(B)}{m(b)}E_B + \frac{m(C)}{m(b)}E_C + \frac{2\sqrt{m(B)m(C)}}{m(b)}\sqrt{E_BE_C}\cos\theta_{BC}, \quad (1)$$

where  $\theta_{BC}$  is the angle between  $\mathbf{P}_B$  and  $\mathbf{P}_C$  in our case  $\cos\theta_{BC}=1$ . This equation in velocity units is:

$$E_b = \frac{m^2(B)}{2m(b)}v_B^2 + \frac{m^2(C)}{2m(b)}v_C^2 + \frac{2m(B)m(C)}{m(b)}v_Cv_B. \quad (2)$$

The calculations have been carried out for the:  $^{36}\text{Ar}+^{24}\text{Mg} \rightarrow ^{24}\text{Mg} + (^{36}\text{Ar} \rightarrow ^{28}\text{Si}+2\alpha)$  reaction,

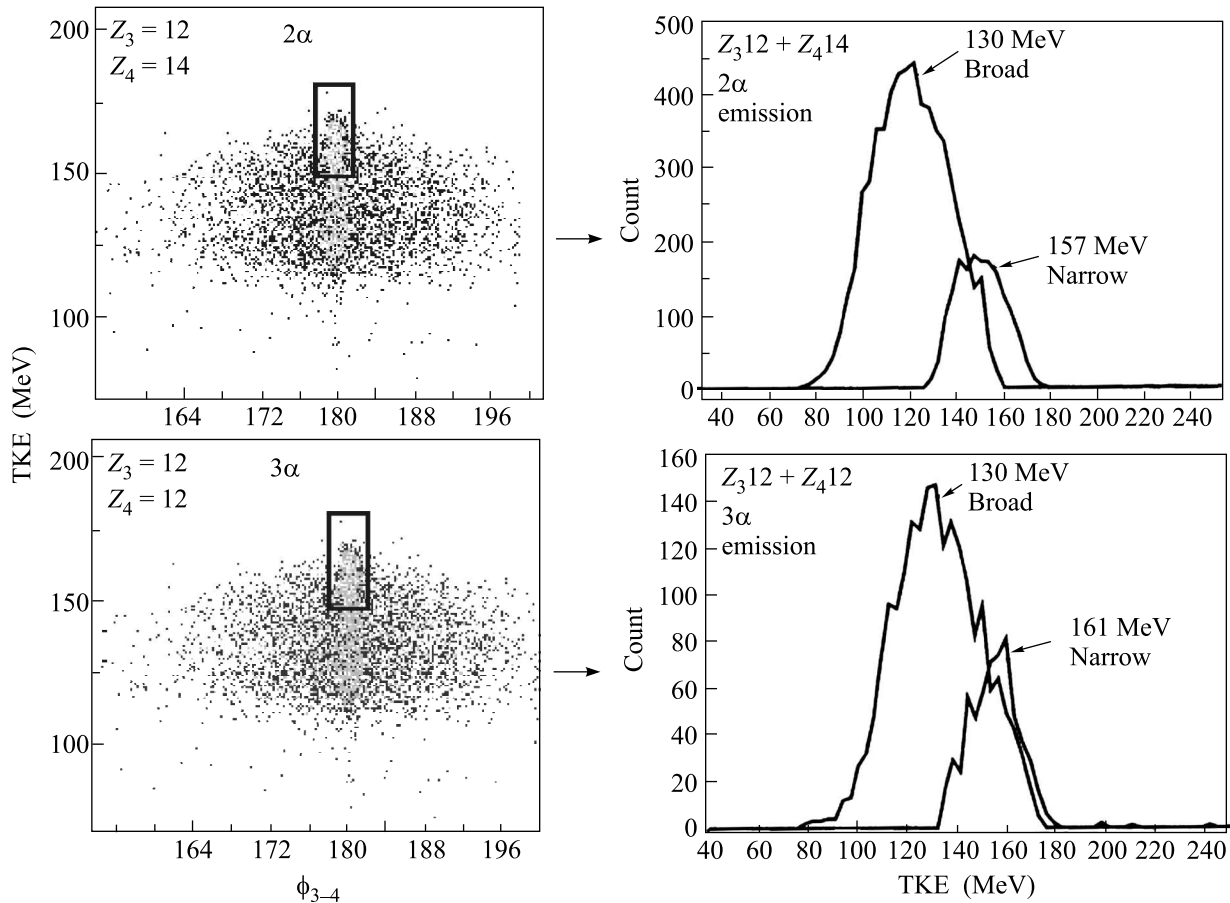


Fig.4. Two dimensional out-of-plane  $\varphi_{3-4}$  vs. TKE distributions (left part) and the projection of TKE with two separated components (right part) for coincident fragments with charges  $Z_3$  and  $Z_4$ . The gates are applied on the narrow parts, which are used for the determination of the total kinetic energy in ternary cluster decay. The broad component represents the statistical binary decay with random  $\alpha$ -particle emission from the excited fragments

where the kinetic energy ( $E_b$ ) of the  $^{24}\text{Mg}$ , and then the TKE process have been calculated. The velocities  $v_B$ ,  $v_C$  and energy  $E_B$  are obtained from the first step and we assume that  $\mathbf{P}_b = -\mathbf{P}_c$ .

From the calculations (in the cm frame) we found that in the mentioned model for ternary fission as a sequential process, the TKE values are 23 MeV larger as compared to the average value of TKE of the fragments produced in the binary decay processes with the random emission of  $\alpha$ -particles from the moving fragments. If we suppose that the narrow part in the two dimensional out-of-plane distribution is connected with considered two-steps process of compound nucleus decay, we can compare calculations by formula (2) with experimental data. Of course, the energy in experimental data was obtained in the lab. system, but the difference between TKE of the ternary fission and  $\alpha$  evaporation processes can be compared with calculations for TKE in the cm frame. Using the special gates (see Fig.4, left

part), we have separated the narrow and broad components in the experimental data in two parts and have observed, that the average difference of TKE between narrow and broad part is approximately 27 MeV (see Fig.4, right part, top). This value agrees with the calculations according to equation (2). In the same way were made calculations for  $3\alpha$ -cluster decay:  $^{36}\text{Ar} + ^{24}\text{Mg} \rightarrow ^{24}\text{Mg} + (^{36}\text{Ar} \rightarrow ^{24}\text{Mg} + 3\alpha)$ . From equation (2) we predict, that the TKE of the fragments (when  $3\alpha$  clusters are forming), are 30 MeV higher as compared to the average value in the binary decay with  $3\alpha$  emission from fragments. This is again in a good agreement with the experimental observations, where the difference is 31 MeV, see Fig.4 right part, bottom. From these results we can conclude that the collinear geometry describes the values of the TKE in an appropriate way.

We have also investigated the yield systematic of the two fragment coincidences as a function of the charge asymmetry for the different values of the missing charge

$\Delta Z$ , where yields for the broad and narrow parts of out-of-plane distribution are obtained (the results are given in ref. [15]). Here a strong odd-even effect in the yield distributions has been observed.

The present work shows, that the narrow and broad out-of-plane correlations can be understood to originate from two different reactions mechanisms. The comprehensive observation of the exclusive narrow coplanar fission-fragment coincidences in our work is a unique feature, which can only be observed with described experimental set-up. We also conclude that the collinear ternary decay processes is the most probable fission mode and is observed due to the formation of elongated hyper-deformed configurations, which arise in the decay compound nuclei at high angular momentum.

V.I.Zherebchevsky thanks the DAAD for a grant.

- 
1. H. J. Wiebecke and M. Zhukov, Nucl. Phys. Nucl. Phys. A **351**, 321 (1981).
  2. G. Royer and F. Haddad, J. Phys. G **21**, 339 (1995).
  3. G. Royer, J. Phys. G **21**, 249 (1995); also G. Royer, F. Haddad, and J. Mignen, J. Phys. G **18**, 2015 (1992).
  4. S. Cohen, F. Plasil, and W. J. Swiatecki, Ann. Phys. (N.Y.) **82**, 557 (1974).
  5. J. Zhang, A. C. Merchant, and W. D. M. Rae, Phys. Rev. C **49**, 562 (1994), and W. D. M. Rae in *Proc. 5<sup>th</sup> Intern. Conf. on Clustering Aspects in Nuclear and Subnuclear Systems 1988*, Kyoto, Prog. Theor. Phys. (Jap.) Ed. K. Ikeda, 1989, p. 80.
  6. G. Leander and S. E. Larsson, Nucl. Phys. A **239**, 93 (1975).
  7. S. Aberg, H. Flocard, and W. Nazarewicz, Ann. Rev. Nucl. Science, **40**, 439 (1990).
  8. S. Aberg and L. O. Joensson, Z. Phys. A **349**, 205 (1994).
  9. I. Ragnarsson, S. Aberg, and R. K. Sheline, Phys. Scr. **24**, 215 (1981); I. Ragnarsson, S. G. Nilsson, and R. K. Sheline, Phys. Rep. **45**, 1 (1978).
  10. C. Beck and A. Szanto de Toledo, Phys. Rev. C **53**, 1989 (1996).
  11. B. Gebauer et al., in Proc. Int. Conf. on the Future of Nucl. Spectroscopy, Crete, Greece, 1993, Eds. W. Gelletly et al., p. 168.
  12. B. Gebauer et al., *Achievements with the Euroball spectrometer*, 2003, Eds. W. Korten and S. Lunardi, p. 135.
  13. S. J. Sanders, A. Szanto de Toledo, and C. Beck, Phys. Rep. **311**, 487 (1999) and references therein.
  14. Sl. Cavallaro et al., Phys. Rev. C **57**, 731 (1998) and references therein.
  15. V. I. Zherebchevsky, W. von Oertzen et al., Phys. Lett. B **2006**, in press.